nature medicine

Normalization of obesity-associated insulin resistance through immunotherapy

Shawn Winer[1,5], Yin Chan[1,5], Geoffrey Paltser[1], Dorothy Truong[1], Hubert Tsui[1], Jasmine Bahrami[2], Ruslan Dorfman[4], Yongqian Wang[4], Julian Zielenski[4], Fabrizio Mastronardi[1], Yuko Maezawa[1], Daniel J Drucker[2], Edgar Engleman[3], Daniel Winer[3] & H.-Michael Dosch[1]

Obesity and its associated metabolic syndromes represent a growing global challenge, yet mechanistic understanding of this pathology and current therapeutics are unsatisfactory. We discovered that CD4$^+$ T lymphocytes, resident in visceral adipose tissue (VAT), control insulin resistance in mice with diet-induced obesity (DIO). Analyses of human tissue suggest that a similar process may also occur in humans. DIO VAT-associated T cells show severely biased T cell receptor V_α repertoires, suggesting antigen-specific expansion. CD4$^+$ T lymphocyte control of glucose homeostasis is compromised in DIO progression, when VAT accumulates pathogenic interferon-γ (IFN-γ)-secreting T helper type 1 (T_H1) cells, overwhelming static numbers of T_H2 (CD4$^+$GATA-binding protein-3 (GATA-3)$^+$) and regulatory forkhead box P3 (Foxp3)$^+$ T cells. CD4$^+$ (but not CD8$^+$) T cell transfer into lymphocyte-free Rag1-null DIO mice reversed weight gain and insulin resistance, predominantly through T_H2 cells. In obese WT and *ob/ob* (leptin-deficient) mice, brief treatment with CD3-specific antibody or its F(ab′)$_2$ fragment, reduces the predominance of T_H1 cells over Foxp3$^+$ cells, reversing insulin resistance for months, despite continuation of a high-fat diet. Our data suggest that the progression of obesity-associated metabolic abnormalities is under the pathophysiological control of CD4$^+$ T cells. The eventual failure of this control, with expanding adiposity and pathogenic VAT T cells, can successfully be reversed by immunotherapy.

The incidence of obesity is increasing worldwide, which is quite problematic as it is a high-risk factor for development of the metabolic syndrome—a melange of pathological conditions that include insulin resistance, glucose intolerance and toxicity, hepatic steatosis and dyslipidemia, as well as the risk of developing type 2 diabetes[1]. Type 2 diabetes and obesity both involve genetic and environmental factors[2], which represent a major global cause of morbidity and mortality, as current nonsurgical therapies are inadequate[3].

Together, the above elements contribute to persistent beta cell stress, dysfunction and type 2 diabetes risk. However, progression of metabolic syndrome to overt diabetes is not easily predicted; many patients with metabolic syndrome never convert, whereas some progress only transiently. Likewise, while some obese individuals progress to metabolic syndrome, others only have mild metabolic abnormalities[2,4]. In any case, adipose tissue inflammation is viewed as a promoter of progression, but the underlying mechanisms remain unclear, as does the nature of what limits or halts progression in individuals with persisting metabolic syndrome, as well as what drives type 2 diabetes progression in those who do convert.

Obesity-associated insulin resistance is a core element of type 2 diabetes development. The impairment of insulin sensitivity involves multiple organs, prominently including hypertrophic adipose tissue with an associated rise in serum and tissue levels of fatty acids, adipokines, and proinflammatory molecules such as interleukin-6 (IL-6) and tumor necrosis factor-α (TNF-α)[1,5]. TNF-α can be produced by both adipocytes and, in particular, macrophages[6,7]. Macrophages accumulate in both VAT and subcutaneous adipose tissue (SAT). The roles of fat-resident macrophages in obesity-induced insulin-resistance differ, with VAT being the principal driver of metabolic syndrome progression[8–10].

Macrophage activation is modified by T cells. IFN-γ–secreting T cells (T_H1), as well as those secreting IL-17 (T_H17), enhance macrophage proinflammatory functions by inducing the release of IL-1, IL-6 and TNF-α. In contrast, anti-inflammatory IL-4 and IL-13–secreting T cells (T_H2), as well as CD4$^+$Foxp3$^+$ regulatory T cells, modify macrophage function by inducing their differentiation into anti-inflammatory, IL-10–secreting M2, or 'alternatively activated', macrophages (AAMs)[11,12]. AAMs are characterized by abundant surface expression of macrophage mannose receptor (MMR) and intracellular arginase activity[13]. Increased tissue levels of IL-10 improve insulin sensitivity in liver and fat[14,15], and AAMs in adipose tissue have been shown to normalize some of the metabolic abnormalities associated with diet-induced obesity in animal models[11,15]. Strategies increasing the number of AAMs or cells that induce them (for

[1]Neuroscience & Mental Health Program, Research Institute, The Hospital for Sick Children, University of Toronto Departments of Pediatrics & Immunology, Toronto, Ontario, Canada. [2]Department of Medicine, Samuel Lunenfeld Research Institute, Mount Sinai Hospital, University of Toronto, Toronto, Ontario, Canada. [3]Department of Pathology, Stanford University School of Medicine, Palo Alto, California, USA. [4]Program in Genetics and Genomic Biology, Research Institute, The Hospital for Sick Children, University of Toronto, Toronto, Ontario, Canada. [5]These authors contributed equally to this work. Correspondence should be addressed to H.-M.D. (michael.dosch@me.com).

Received 3 March; accepted 9 June; published online 26 July 2009; doi:10.1038/nm.2001

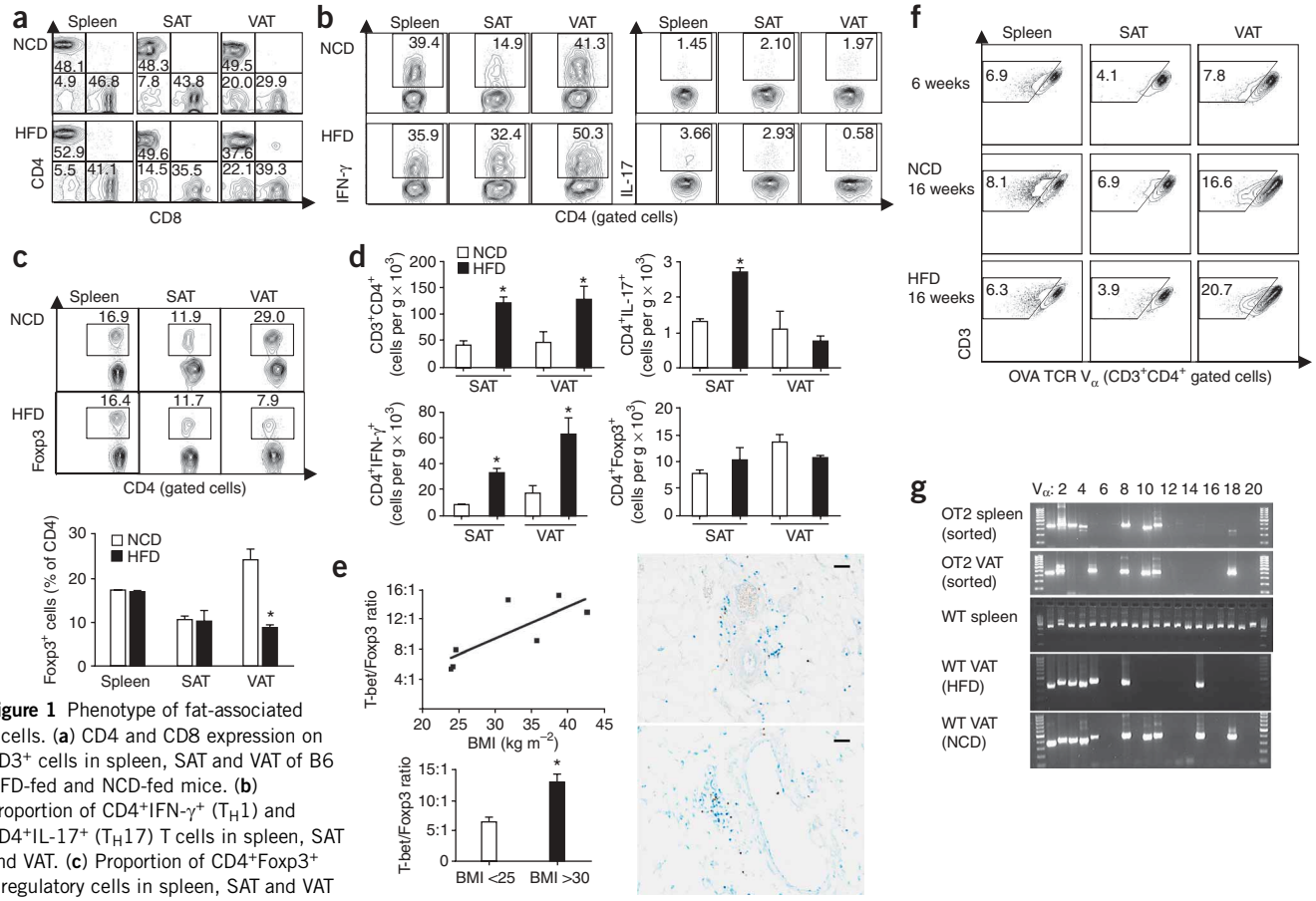

Figure 1 Phenotype of fat-associated T cells. (**a**) CD4 and CD8 expression on $CD3^+$ cells in spleen, SAT and VAT of B6 HFD-fed and NCD-fed mice. (**b**) Proportion of $CD4^+IFN\text{-}\gamma^+$ (T_H1) and $CD4^+IL\text{-}17^+$ (T_H17) T cells in spleen, SAT and VAT. (**c**) Proportion of $CD4^+Foxp3^+$ T regulatory cells in spleen, SAT and VAT (top, FACS plots; bottom, pooled data; $^*P < 0.03$, *t* test). (**d**) Total number of $CD3^+CD4^+$, $CD4^+IFN\text{-}\gamma^+$ (T_H1), $CD4^+IL\text{-}17^+$ (T_H17) and $CD4^+Foxp3^+$ T cells per g of SAT and VAT in NCD-fed and HFD-fed mice ($n = 4$ or 5 per group, $^*P < 0.05$, *t* test). (**e**) Top left, T-bet (T_H1) to Foxp3 ratio in human VAT ($r^2 = 0.62$, $P < 0.05$). Bottom left, VAT T-bet to Foxp3 ratio in humans with BMI >30 versus BMI <25 ($^*P < 0.02$, *t* test). Right, Foxp3 (brown) and T-bet (blue, T_H1 cells) in VAT from humans with BMI >30 (top) or BMI <25 (bottom). Scale bar, 50 μm. T-bet to Foxp3 ratios are from >200 stained cells from two tissue levels. (**f**) Flow cytometric analysis of $CD3^+CD4^+$ T cells (%) with secondary re-rearranged non-OVA TCRα, as detected by their low OT2 TCRα to CD3 ratio in spleens, SAT and VAT of 6- or 16-week-old NCD-fed or HFD-fed B6 OT2 mice. (**g**) Expression of the genes encoding TCR V_α among $CD4^+$ T cells isolated from spleens of 16-week-old obese WT or OT2 mice and from VAT of HFD-fed and NCD-fed WT and OT2 mice. $CD4^+$ OT2 T cells were identified and sorted as in **f**. All mice were 14–16-weeks-old, and each contour plot represents three or four independent experiments. All FACS plots include cell percentages of the corresponding quadrants; histograms represent means ± s.d.

example, T_H2 or $CD4^+Foxp3^+$ T cells) might be of therapeutic promise in insulin resistance and type 2 diabetes.

$CD4^+$ and $CD8^+$ T cells enter VAT and SAT of obese mice and humans[16,17]. The function of these fat-associated T cells and their conceivable roles in obesity, glucose homeostasis or both are unknown, nor are their antigen specificities, activation history or T sublineage profiles known[18].

We investigated the impact of T cells on the glucose homeostasis of C57BL/6 (B6) mice with DIO. We discovered a progressive bias in the recruitment to and expansion of proinflammatory T_H1, but not T_H17 T cells in adipose tissue, with a body mass–dependent, progressive decline in the proportions of anti-inflammatory $CD4^+Foxp3^+$ regulatory T cells observed in obese mice and humans. We used independent experimental model systems in mice to delineate several fat-resident immune elements with distinct impacts on weight gain, insulin resistance and glucose homeostasis. Among these, our observation of VAT-specific T cell receptor bias was most unexpected, as it is typically associated with antigen-specific and/or pathogen-specific T cell expansion as well as autoimmunity[19–22].

The predominant T cell effect on glucose homeostasis, revealed by $CD4^+$ T cell reconstitution studies in lymphocyte-free DIO Rag1-null mice, was improvement of glucose tolerance, enhanced insulin-sensitivity and lessening of weight gain. We identified the subsets involved and probed the overall T cell impact in fully developed DIO, using immunotherapy with a clinically effective CD3-specific antibody or its nonmitogenic $F(ab')_2$ fragment[23]. Both therapies substantially normalized insulin resistance and glucose homeostasis, selectively restoring $CD4^+Foxp3^+$ T cell pools in VAT. Treatment was effective for months after a short course of injections, despite unchanged high-fat diet consumption. These results suggest a dual role of fat-associated T lineage cells, which initially mitigate inflammation-induced insulin resistance until VAT-driven T_H1 expansion overwhelms this protective effect, a process that can be targeted and corrected therapeutically.

RESULTS

Characterization of fat-associated T cells

We characterized the numbers and subsets of fat-associated T cells from inguinal SAT and epididymal VAT of 14- to 18-week-old high-fat diet (HFD)-fed and normal chow diet (NCD)-fed B6 mice, consistently collecting about 4×10^5 $CD3^+$ T cells per g VAT and SAT. The fat-associated T cell subset distribution varied somewhat, with a trend toward higher CD8 to CD4 ratios, in particular in VAT of HFD-fed

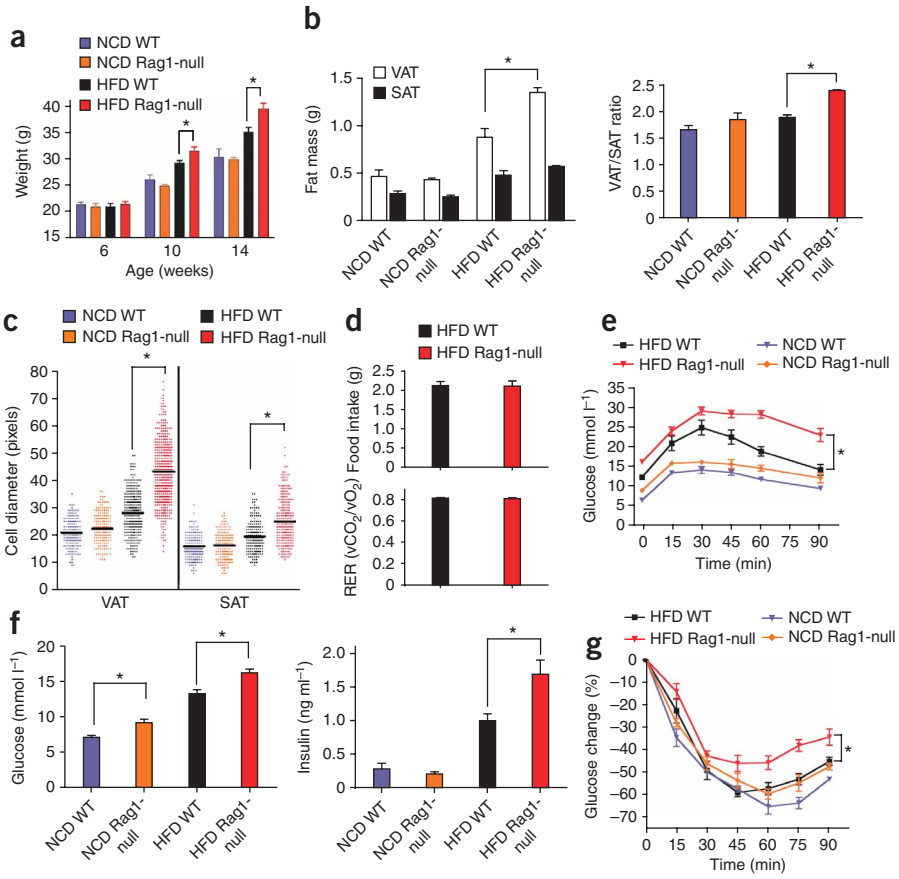

Figure 2 Impact of lymphocyte deficiency on weight gain, fat distribution, glucose tolerance and insulin resistance. (**a**) Body weights of ≥6-week-old WT and Rag1-null B6 mice on NCD ($n = 20$ per group) or HFD ($n = 20$ per group, $^*P < 0.03$, Mann-Whitney, WT versus Rag1-null). (**b**) Weights of single epididymal VAT and inguinal SAT pads from 14- to15-week-old WT and Rag1-null mice on NCD or HFD (left, $n = 6$ mice per group, $^*P < 0.03$, *t* test; right, VAT to SAT ratio, $^*P < 0.001$, *t* test). (**c**) Relative fat cell diameter (see Online Methods, $n = 3$ mice per group, $^*P < 0.0001$, Mann-Whitney). (**d**) Food intake (top) and respiratory exchange ratio (RER, bottom) in HFD-fed WT or Rag1-null mice ($n = 4$ per group). vCO_2, carbon dioxide elimination; vO_2, oxygen consumption. (**e**) Glucose tolerance of Rag1-null or WT mice on NCD or HFD ($n = 10$ per group, $^*P < 0.02$, two-way analysis of variance (ANOVA)). (**f**) Fasting glucose (left) or insulin blood concentrations (right) in 14-week-old HFD-fed and NCD-fed WT or Rag1-null mice ($n = 10$ mice per group, $^*P < 0.05$, *t* test). (**g**) Insulin tolerance test (ITT) in 14-week-old WT Rag1-null mice on NCD or HFD ($n = 6$–10 per group, $^*P < 0.05$, two-way ANOVA). All histograms represent means ± s.d.

mice compared to VAT of regular diet controls (**Fig. 1a**). VAT from lean and obese mice also contained pools of $CD3^+CD4^-CD8^-$lymphocytes (that is, natural killer (NK), NKT and Tγ/δ lineage cells)[24], and these were largely unaffected by obesity (**Fig. 1a**).

$CD4^+$ effector T cells can generally be subdivided into proinflammatory cells (T_H1, T_H17) and anti-inflammatory and regulatory sublineages (T_H2, $Foxp3^+$). There were fewer IFN-γ–secreting T_H1 cells in SAT than in VAT from NCD and HFD B6 mice (**Fig. 1b**). HFD generated a progressive IFN-γ bias among fat-associated T cells, whereas it diminished the small VAT T_H17 sublineage (**Fig. 1b**). Compared to VAT of NCD-fed mice, the proportion of regulatory $CD4^+Foxp3^+$ T cells in VAT from HFD-fed mice was 70% lower, probably contributing to the proinflammatory VAT profiles of obese mice (**Fig. 1c**). The ratio of T_H1 to $Foxp3^+$ T cells in VAT increased from ∼1.5:1 in NCD-fed mice to ∼6.5:1 in DIO mice. In terms of absolute numbers, approximately three times more T_H1 cells accumulated per gram of fat in HFD-fed mice (**Fig. 1d**), whereas numbers of $CD4^+Foxp3^+$ T cells per g of VAT varied little (**Fig. 1d**). The numbers of T_H1 cells in adipose tissue thus represent the dynamic variable affected by diet-induced obesity. The high proportion of $CD4^+Foxp3^+$ T cells in VAT of lean mice, which are progressively diluted by IFN-γ–producing cells in progressive DIO, suggests one candidate cellular mechanism by which progressive obesity leads to worsening metabolic control.

Observations in lean and obese humans were strikingly analogous. In VAT from obese humans (**Fig. 1e**), T_H1 cells that express the lineage-specific Tbet transcription factor[25] outnumbered $Foxp3^+$ T cells with a ratio of ∼12:1, whereas the ratio was ∼6:1 in VAT of lean humans (**Fig. 1e**). The relative proportion of T_H1 to $Foxp3^+$ cells in VAT correlated with body mass index (BMI) (**Fig. 1e**, $r^2 = 0.62$). As in mice, we observed human fat-associated T cells clustered around blood vessels, some scattered between adipocytes (**Supplementary Fig. 1a**). We commonly observed $Foxp3^+$ fat-associated T cells in close proximity to monocytes and macrophages (**Supplementary Fig. 1b**), predicting possible interactions with fat-associated monocytes and macrophages.

Tissue-selective lymphocyte accumulation can reflect a number of mechanisms, including cognate events, involving T cell receptor engagements with its major histocompatibility complex–antigen conjugates. Although we did not expect to find selective T cell receptor (TCR) engagement of VAT-associated T cells, we decided to formally rule this possibility out by using ovalbumin (OVA)-specific, OT2 TCR transgenic mice[26]. These B6 mice developed metabolic complications of DIO (**Supplementary Fig. 2a–c**). A small proportion of transgenic OT2 T cells can bypass TCRα allelic exclusion and undergo random, secondary V_α rearrangements, yielding a second surface TCR that can recognize non-OVA antigens[27]. Such cells can be identified through their reduced surface expression of the original, transgenic TCR V_α relative to CD3.

There were small pools (4–7%) of T cells with secondary TCRα rearrangements in spleens, VAT and SAT of young OT2 mice (**Fig. 1f**). Beginning at around 6 weeks of age, secondary TCRα rearrangements slowly and selectively increased thereafter (7–21%) in VAT of all mice, but, in particular, in HFD-fed OT2 mice (**Fig. 1f**). This VAT tissue-specific effect indicates a strong selective pressure toward a non-OVA antigen(s); that is, an adipose tissue antigen or antigen modification present only in VAT but not in SAT or elsewhere. Thus, unexpectedly, T cell expansion in VAT seems, at least in part, antigen driven.

We sought further support for this notion and PCR amplified each of the 20 TCR V_α–encoding genes in highly purified T cells with secondary TCR V_α rearrangements. These cells had been sorted by FACS from spleens and VAT of obese, 16-week-old OT2 mice; wild-type (WT) B6 spleens served as controls that expressed the expected

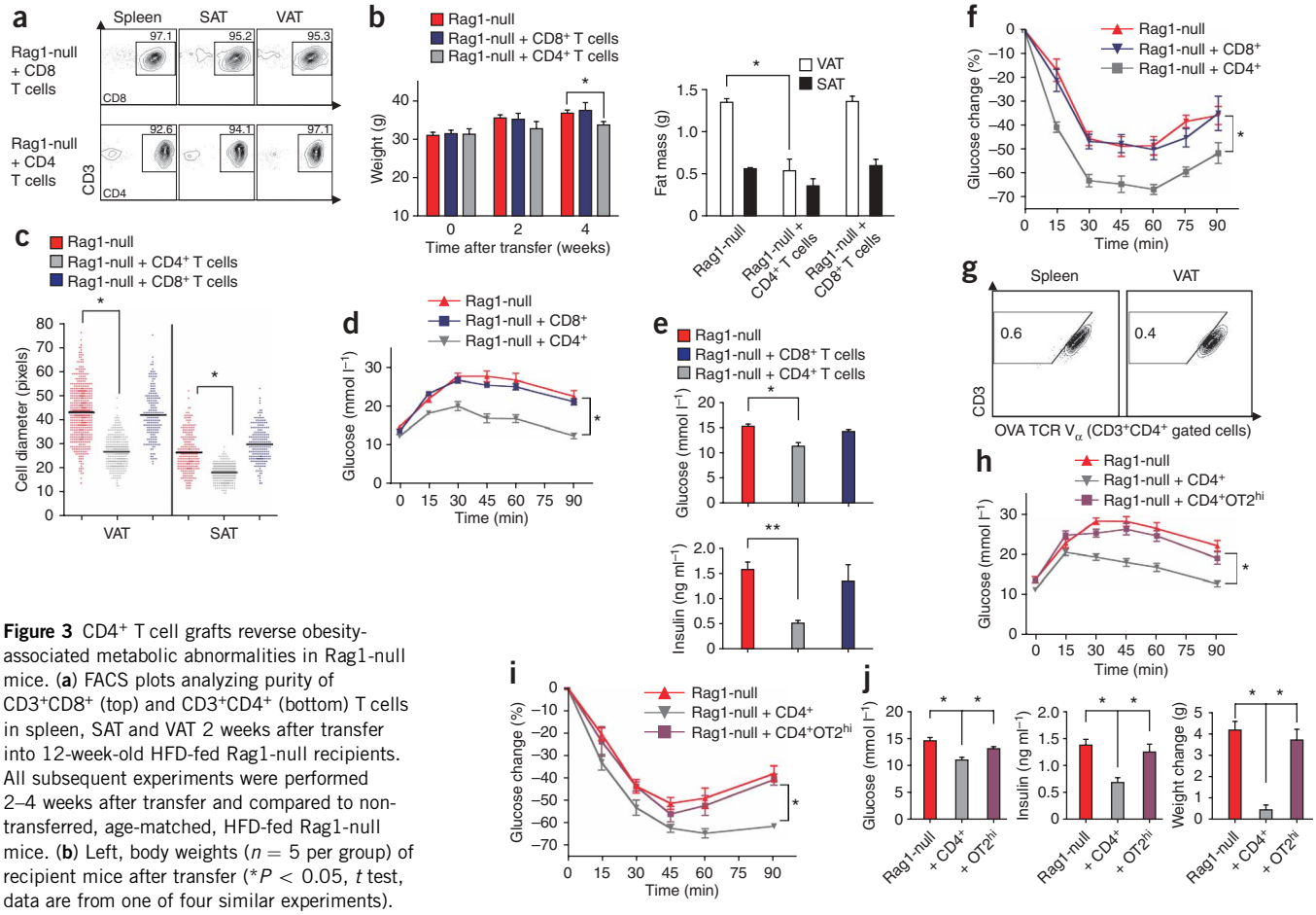

Figure 3 CD4+ T cell grafts reverse obesity-associated metabolic abnormalities in Rag1-null mice. (**a**) FACS plots analyzing purity of $CD3^+CD8^+$ (top) and $CD3^+CD4^+$ (bottom) T cells in spleen, SAT and VAT 2 weeks after transfer into 12-week-old HFD-fed Rag1-null recipients. All subsequent experiments were performed 2–4 weeks after transfer and compared to non-transferred, age-matched, HFD-fed Rag1-null mice. (**b**) Left, body weights ($n = 5$ per group) of recipient mice after transfer ($^*P < 0.05$, *t* test, data are from one of four similar experiments). Right, weights of individual VAT and SAT pads ($n = 5$ per group); $^*P < 0.05$, *t* test. (**c**) Adipocyte diameter after transfer of $CD4^+$ or $CD8^+$ T cells into HFD-fed Rag1-null mice ($n = 3$ mice per group, $^*P < 0.01$, Mann-Whitney). (**d**) Glucose tolerance in HFD-fed Rag1-null recipients after $CD4^+$ T cell transfer, $CD8^+$ T cell transfer or no transfer ($n = 10$ per group, $^*P < 0.0001$, two-way ANOVA). (**e**) Fasting glucose (top) and insulin (bottom) in $CD4^+$ or $CD8^+$ T cell-transferred HFD-fed Rag1-null mice ($n = 5$–10 mice per group, $^*P < 0.03$, $^{**}P < 0.01$, *t* test). (**f**) Insulin tolerance in HFD-fed Rag1-null mice reconstituted with $CD4^+$ T cells, $CD8^+$ T cells or nonreconstituted controls ($n = 10$, $^*P < 0.05$, two-way ANOVA). (**g**) FACS plots of OT2 TCR V_α rearrangements in spleen and VAT, 2 weeks after transfer. The purity of $CD4^+OT2^{hi}$ cells transferred was 99.5%. (**h**,**i**) Glucose tolerance test (**h**) and insulin tolerance test (**i**) after transfer of $CD4^+$ OT2 $TCR\alpha^{hi}$ ($CD4^+OT2^{hi}$) T cells or $CD4^+$ T cells into HFD-fed Rag1-null mice ($n = 5$ per group, $^*P < 0.0001$, two-way ANOVA). (**j**) Fasting glucose (left) and fasting insulin (middle) in $CD4^+$ or $CD4^+$ OT2 $TCR\alpha^{hi}$ ($OT2^{hi}$)-transferred HFD-fed Rag1-null mice ($n = 5$ mice per group, $^*P < 0.05$, *t* test). Right, weight gain after transfer of $CD4^+$ or $CD4^+$ $OT2^{hi}$ $TCR\alpha^{hi}$ T cells into HFD-fed Rag1-null mice ($n = 5$ mice per group, $^*P < 0.004$, *t* test). All FACS plots include cell percentages of the corresponding quadrants; histograms represent means ± s.d.

full spectrum of TCRα families (**Fig. 1g**). TCR V_α usage in spleen and VAT T cells from obese OT2 mice differed substantially; only some of the receptors were systemically shared, including the transgenic $V_{\alpha 2}$ (**Fig. 1g**). VAT T cells had lost $V_{\alpha 3}$ but gained strong expression of $V_{\alpha 5}$ and $V_{\alpha 18}$ (**Fig. 1g**). Spectra-typing of the CDR3 region in OT2 TCRα-encoding genes emphasized the strong selection pressures in VAT for very narrow TCRα diversity and negative pressure against selection of the majority of systemic TCR V_αs, thus generating an impressive TCR V_α bias among VAT T cells, which includes unique $V_{\alpha 5}$ (417 base pairs) and $V_{\alpha 18}$ (393 base pairs) regions (**Supplementary Fig. 3**).

Motivated by the VAT tissue–specific TCR selection bias and to rule out possible effects of the TCR transgene, we repeated this analysis but included sorted $CD4^+TCR\beta^+NK1.1^-$ VAT T cells from HFD-fed as well as NCD-fed B6 WT mice (**Fig. 1g**). We observed a strong TCR V_α bias in VAT of lean (10 of 20 TCR V_α families expressed) and, more so, in VAT of HFD-fed mice (only seven of the same ten V_α families used in lean mice) (**Fig. 1g**). Spectra-typing of the CDR3 region showed markedly altered diversity in VAT TCR V_α repertoires of DIO versus lean B6 mice (**Supplementary Fig. 4**). These results suggest antigen-specific expansion of T cell repertoires in VAT of lean mice, with increasing bias in progressive obesity, probably driven by adipose tissue changes that occur as a result of obesity. Tissue-driven TCR bias is common in organ-selective autoimmune disorders[19–22]. However, this process has not previously been associated with obesity or type 2 diabetes, and will require identification of the relevant tissue self epitopes to formally prove autoreactivity.

Metabolic role of T cells in obesity

HFD-fed Rag1-null mice lack lymphocytes, gain more weight and show greater visceral adiposity than HFD-fed WT mice (**Fig. 2a**,**b**). Increased visceral obesity in HFD-fed Rag1-null mice was mostly due to notable adipocyte hypertrophy (**Fig. 2c** and **Supplementary Fig. 5**). There were no significant abnormalities in body weight, adipose tissue mass or adipocyte size in Rag1-null mice on NCD (**Fig. 2a–c**), nor were there differences in food intake, CO_2 output or O_2 consumption between HFD-fed Rag1-null and HFD-fed WT mice (**Fig. 2d**).

Glucose and insulin tolerances in 14-week-old, HFD-fed Rag1-null mice were severely impaired, with fasting glucose at diabetic levels (**Fig. 2e**,**f**), fasting hyperinsulinemia (**Fig. 2f**) and low insulin sensitivity upon insulin challenge (**Fig. 2g**). Rag1-null mice on NCD showed nonsignificant trends toward poorer glucose tolerance and increased insulin resistance. However, a significant elevation of fasting blood glucose (**Fig. 2e–g**) implies that the metabolic role of lymphocytes may be physiological and occurs even in the absence of a hypercaloric diet.

CD4$^+$ T cells regulate obesity and glucose homeostasis

The DIO Rag1-null phenotype delineated an overall protective role of lymphocytes in weight gain and insulin resistance. To identify lymphocyte subsets involved in this process, we reconstituted 12-week-old HFD-fed Rag1-null mice with 5×10^6 CD4$^+$ or CD8$^+$ T cells, each specifically depleted of CD49b$^+$ NK and NKT cells, CD11b$^+$ monocytes and macrophages and CD19$^+$ and CD45R$^+$ B cells before transfer.

Two weeks after transfer, the cells had populated spleen, SAT and VAT with high purity (~95%, **Fig. 3a**). CD4$^+$ (but not CD8$^+$) T cell reconstitution lowered weight gain quite notably by 2–4 weeks after transfer (**Fig. 3b**), despite similar food intake, CO_2 output and O_2 consumption in all mice (**Supplementary Fig. 6a**,**b**). Lesser weight gain was apparent in SAT and, even more so, in VAT (**Fig. 3b**), and it was associated with smaller adipocyte size in both fat compartments (**Fig. 3c** and **Supplementary Fig. 5**), when CD4$^+$ T cell-transferred HFD-fed Rag1-null recipients were compared to CD8$^+$ T cell–transferred HFD-fed Rag1-null recipients or Rag1-null control mice. CD4$^+$ T cell transfer also lowered serum levels of obesity-associated adipokines such as leptin, resistin and monocyte chemoattractant protein-1

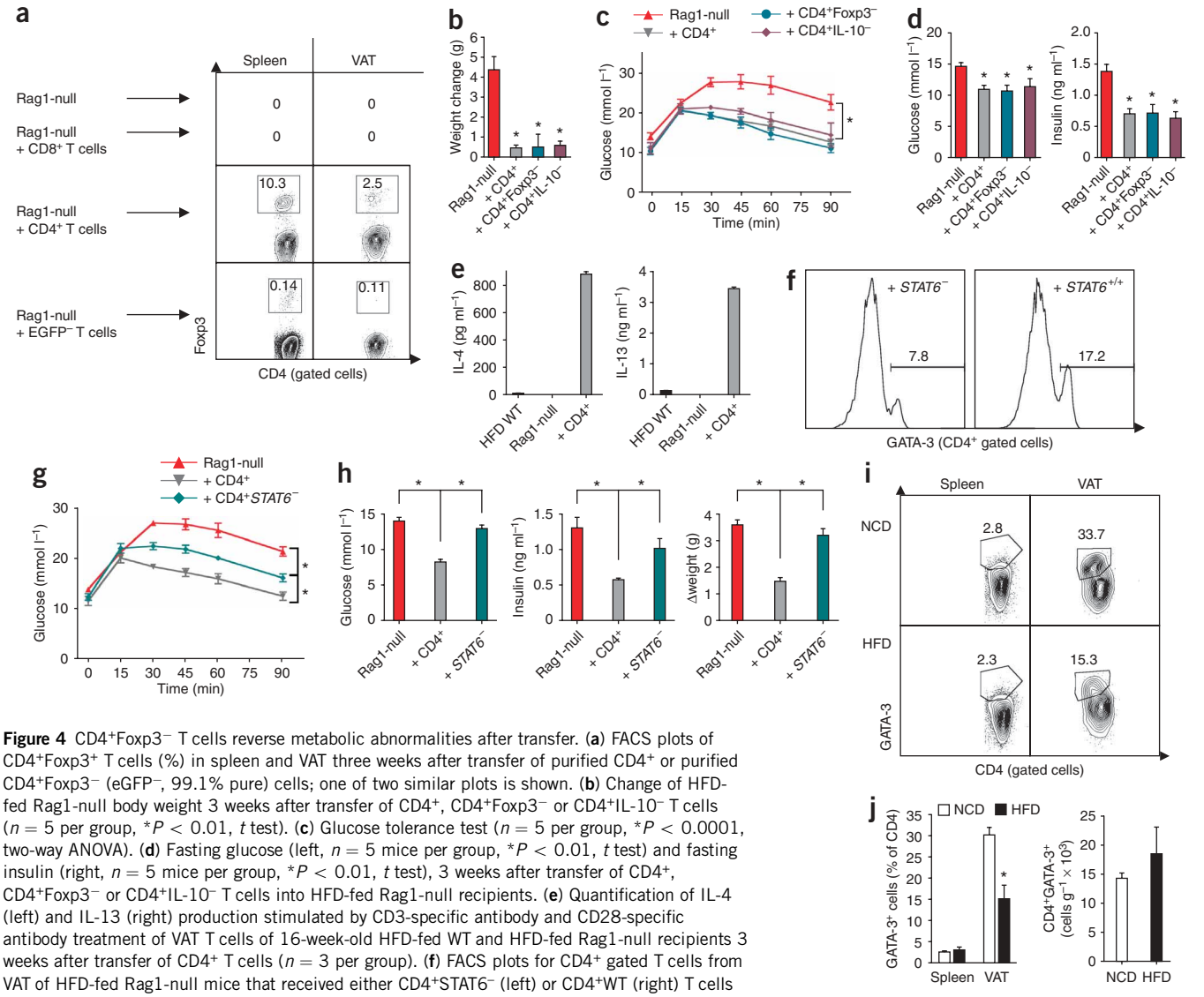

Figure 4 CD4$^+$Foxp3$^-$ T cells reverse metabolic abnormalities after transfer. (**a**) FACS plots of CD4$^+$Foxp3$^+$ T cells (%) in spleen and VAT three weeks after transfer of purified CD4$^+$ or purified CD4$^+$Foxp3$^-$ (eGFP$^-$, 99.1% pure) cells; one of two similar plots is shown. (**b**) Change of HFD-fed Rag1-null body weight 3 weeks after transfer of CD4$^+$, CD4$^+$Foxp3$^-$ or CD4$^+$IL-10$^-$ T cells ($n = 5$ per group, $^*P < 0.01$, t test). (**c**) Glucose tolerance test ($n = 5$ per group, $^*P < 0.0001$, two-way ANOVA). (**d**) Fasting glucose (left, $n = 5$ mice per group, $^*P < 0.01$, t test) and fasting insulin (right, $n = 5$ mice per group, $^*P < 0.01$, t test), 3 weeks after transfer of CD4$^+$, CD4$^+$Foxp3$^-$ or CD4$^+$IL-10$^-$ T cells into HFD-fed Rag1-null recipients. (**e**) Quantification of IL-4 (left) and IL-13 (right) production stimulated by CD3-specific antibody and CD28-specific antibody treatment of VAT T cells of 16-week-old HFD-fed WT and HFD-fed Rag1-null recipients 3 weeks after transfer of CD4$^+$ T cells ($n = 3$ per group). (**f**) FACS plots for CD4$^+$ gated T cells from VAT of HFD-fed Rag1-null mice that received either CD4$^+$STAT6$^-$ (left) or CD4$^+$WT (right) T cells 3 weeks previously. (**g**) Glucose tolerance 3 weeks after transfer of CD4$^+$ or CD4$^+$STAT6$^-$ T cells ($n = 5$ per group, $^*P < 0.05$, two-way ANOVA). (**h**) Fasting glucose (left), fasting insulin (middle) and weight change (right) in HFD-fed Rag1-null recipients 3 weeks after transfer of purified CD4$^+$ or CD4$^+$STAT6$^-$ T cells ($n = 5$ mice per group, $^*P < 0.01$, t test). (**i**) Representative FACS plot of CD4$^+$GATA-3$^+$ (%T_H2) cells in spleen and VAT of 14- to 16-week-old NCD-fed and HFD-fed B6 mice. (**j**) Left, pooled data from **i** ($n = 4$ per group, $^*P < 0.03$, t test). Right, total number of CD4$^+$GATA-3$^+$ (T_H2) T cells per g of VAT in NCD-fed and HFD-fed B6 mice ($n = 4$ per group, $P > 0.4$, t test). All FACS plots include cell percentages of the corresponding quadrants; histograms represent means ± s.d.

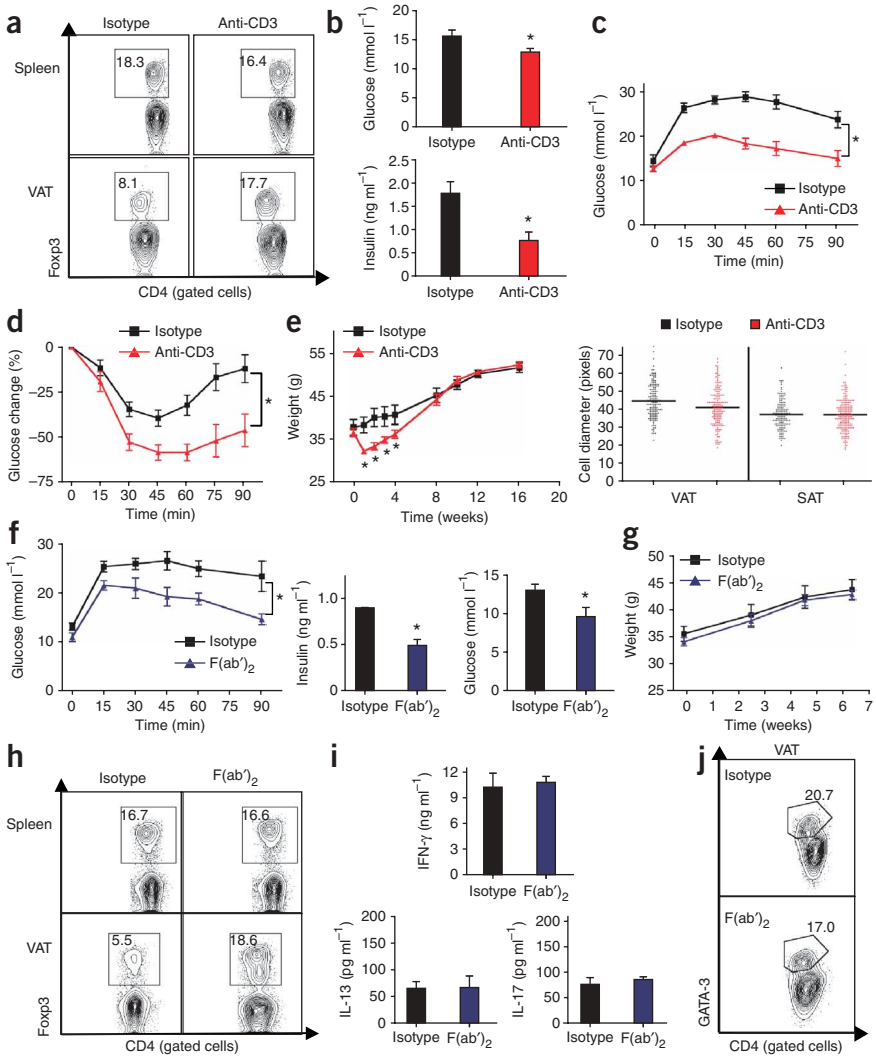

Figure 5 CD3-specific antibody and its F(ab′)$_2$ fragment improve obesity-induced insulin resistance. Sixteen-week-old obese (HFD) B6 mice received CD-3–specific antibody (anti-CD3, **a–e**), isotype-matched control IgG or CD3-specific F(ab′)$_2$ (F(ab′)$_2$, **f–j**), maintaining HFD for 6 or 9 weeks. (**a**) FACS plots (%) of CD4$^+$Foxp3$^+$ T cells in spleen and VAT 9 weeks after CD3-specific antibody treatment (one of three similar experiments is shown). (**b**) Fasting glucose (top) and insulin (bottom) after CD3-specific antibody treatment ($n = 8$, $^*P < 0.05$, t test). (**c**,**d**) Glucose tolerance (**c**, $n = 8$, $^*P < 0.0004$, two-way ANOVA) and ITT (d, $n = 8$, $^*P < 0.0005$, two-way ANOVA) after CD3-specific antibody treatment. (**e**) Left, body weights of HFD-fed mice after CD3-specific antibody treatment ($n = 8$, $^*P < 0.05$, t test). Right, adipocyte diameter after CD3-specific antibody treatment ($n = 3$ mice per group). (**f**) Glucose tolerance (left) ($n = 5$, $^*P < 0.01$, two-way ANOVA, one of two similar experiments), fasting insulin (middle) and fasting glucose (right) in HFD-fed mice ($n = 5$, $^*P < 0.04$, t test) 6 weeks after F(ab′)$_2$ treatment. (**g**) Body weights of HFD-fed mice after F(ab′)$_2$ treatment. (**h**) CD4$^+$Foxp3$^+$ T cells in spleen and VAT of HFD-fed B6 mice 6 weeks after F(ab′)$_2$ treatment (one of three similar experiments). (**i**) IFN-γ, IL-17 and IL-13 concentrations after stimulation of B6 VAT T cells with CD3-specific antibody plus CD28-specific antibody 8 weeks after F(ab′)$_2$ treatment ($n = 3$ per group). (**j**) FACS plot of CD4$^+$ gated, GATA-3–stained VAT T cells 8 weeks after F(ab′)$_2$ treatment. All FACS plots include cell percentages of the corresponding quadrants; histograms represent means ± s.d.

(MCP-1) (**Supplementary Fig. 6c**), and it normalized glucose tolerance, with lower fasting insulin and glucose levels and improved insulin sensitivity within 2 weeks (**Fig. 3d–f**).

To determine the role of cognate, TCR-dependent events, we purified OVA-specific T cells from OT2 TCR-transgenic B6 mice by sorting cells without secondary rearrangements. Two weeks after adoptive transfer of these CD4$^+$ OT2 TCR V$_\alpha^{hi}$ lymphocytes into HFD-fed Rag1-null mice, there were still almost no T cells with secondary rearrangements in spleens or fat (**Fig. 3g**). Notably, the presence of exclusively OVA-specific T cells in VAT failed to improve glucose tolerance (**Fig. 3h**), insulin sensitivity (**Fig. 3i**), fasting blood glucose (**Fig. 3j**), fasting insulin (**Fig. 3j**) or body weight (**Fig. 3j**). These results indicate that CD4$^+$ T cells in VAT mediate the positive global controls of DIO-associated metabolic abnormalities in an antigen-specific fashion.

CD4$^+$Foxp3$^+$ T cells are regulators of inflammation, and CD4$^+$ T cell transfer into HFD-fed Rag1-null mice slowly repopulated Rag1-null VAT with CD4$^+$Foxp3$^+$ T cells, by 2–3% 2 weeks after transfer (**Fig. 4a**). To determine whether CD4$^+$Foxp3$^+$ T cells are essential in the regulation of glucose homeostasis after cell transfer, we sorted and transferred CD4$^+$Foxp3$^-$ T cells, using the bicistronic, Foxp3-eGFP–transgenic B6 mouse line, in which Foxp3$^+$ cells co-express the fluorescent green marker[28].

Transferred Foxp3$^-$CD4$^+$ T cells showed little (~0.1%) conversion to CD4$^+$Foxp3$^+$ cells in spleen or VAT (**Fig. 4a**), but recipient mice were as protected from weight gain as mice receiving full CD4$^+$ T cell grafts from WT hosts (**Fig. 4b**). CD4$^+$Foxp3$^-$ T cells were equally sufficient to improve glucose tolerance, fasting glucose and fasting insulin concentrations (**Fig. 4c,d**), suggesting that metabolic control after CD4$^+$ T cell transfer does not require CD4$^+$Foxp3$^+$ regulatory T cell function in our adoptive transfer model. Regulatory T cells and inducible type 1 regulatory T cells produce IL-10, a major anti-inflammatory cytokine, as part of their effector function[29]. Adoptive transfer of CD4$^+$ T cells from IL-10–null B6 mice was as protective as full WT CD4$^+$ grafts, indicating that T cell–derived IL-10 is dispensable for the beneficial effects of CD4$^+$ T cells (**Fig. 4b–d**).

T cells can acquire a T$_H$2 profile during the extensive homeostatic expansion that occurs after transfer into Rag1-null mice, and we observed considerable T$_H$2 cytokine production (IL-4 and IL-13) in VAT-derived T cells of HFD-fed Rag1-null CD4$^+$ T cell recipients (**Fig. 4e**). Maintenance of T$_H$2 cells is largely dependent on signal transducer and activator of transcription-6 (STAT6), and STAT6 deficiency severely impairs, without completely ablating the T$_H$2 sublineage, which can be identified by the GATA-3 transcription factor[30–32]. To determine the role of T$_H$2 cells in our transfer model, we transferred CD4$^+$STAT6-null T cells into HFD-fed Rag1-null mice. As expected, recipients of CD4$^+$STAT6-null T cells generated reduced numbers of CD4$^+$GATA-3$^+$ (T$_H$2) T cells in VAT compared to mice

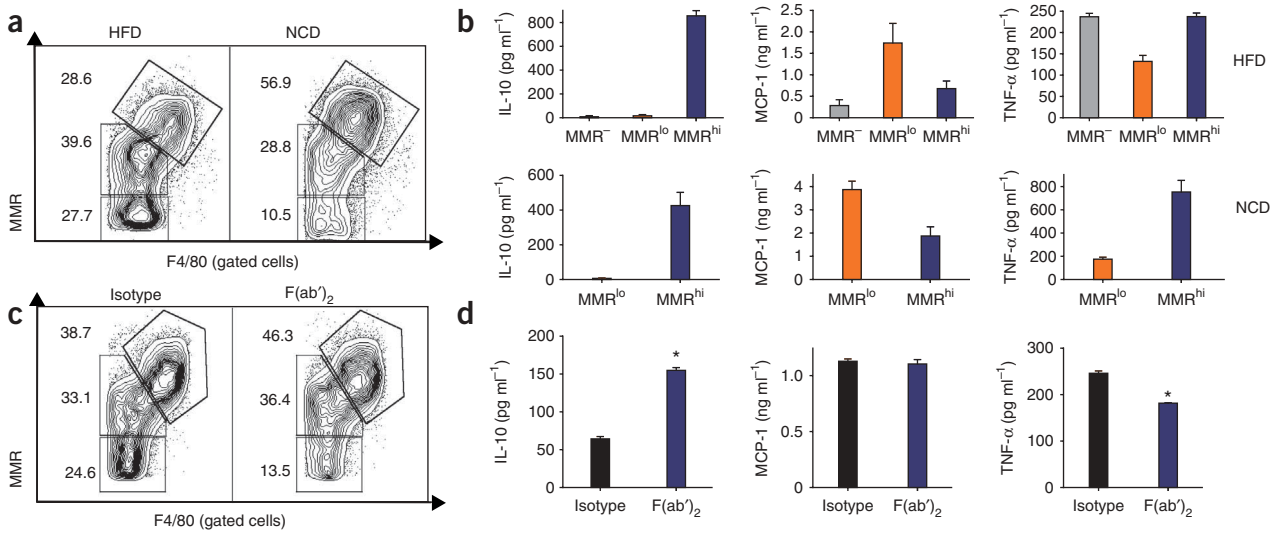

Figure 6 F(ab′)$_2$ therapy alters VAT-resident macrophage phenotype. (**a**) MMR^{hi} (%, top gate), MMR^{lo} (middle gate) and MMR^{-} (bottom gate) macrophages from VAT of 16-week-old HFD-fed or lean NCD-fed B6 mice (representative data from four similar experiments). (**b**) Quantification of IL-10 (left), MCP-1 (middle) and TNF-α (right) produced by lipopolysaccharide (LPS)-stimulated F4/80^{+} macrophages sorted from VAT of HFD-fed (top) or NCD-fed (bottom) mice into MMR^{-}, MMR^{lo} and MMR^{hi} cell populations (one of four similar experiments). We consistently failed to obtain sufficient cell numbers for analysis of MMR^{-} macrophages from VAT from lean mice. (**c**) FACS plots from two independent experiments measuring MMR expression in F4/80^{+} macrophages from HFD-fed B6 VAT 6 weeks after F(ab′)$_2$ treatment. (**d**) Quantification of IL-10 (left), MCP-1 (middle) and TNF-α (right) produced by LPS-stimulated F4/80^{+} macrophages sorted from VAT 6 weeks after F(ab′)$_2$ treatment ($n = 3$ per group, $^{*}P < 0.05$, *t* test). All FACS plots include cell percentages of the corresponding quadrants; histograms represent means ± s.d.

receiving WT CD4^{+} T cells (**Fig. 4f**). CD4^{+}STAT6-null T cells lacked most of the positive CD4^{+} impact on glucose tolerance, fasting glucose, fasting insulin and weight gain, identifying metabolic effects of T$_H$2 cells in the CD4^{+} T cell transfer model (**Fig. 4g,h**).

The implication of T$_H$2 cells, as regulators of glucose homeostasis in the transfer model, prompted us to compare this subset in VAT of NCD-fed and HFD-fed WT mice (**Fig. 4i,j**). The proportions of T$_H$2 (CD4^{+}GATA-3^{+}) cells were significantly lower (~50%) in VAT of HFD-fed mice (**Fig. 4i,j**); however, the absolute numbers of T$_H$2 cells/gram of VAT remained fairly constant (**Fig. 4j**). As is the case with CD4^{+}Foxp3^{+} T cells, our results suggest that smaller T$_H$2 cell proportions in DIO-associated VAT represent a candidate mechanism for worsening metabolic control in progressively obese mice, and strategies that increase VAT T$_H$2 cell content might be of therapeutic benefit.

Immunotherapy of insulin resistance

The various DIO-associated metabolic parameters relevant here are complex, and immune controls probably involve multiple levels and mechanisms. Although the scarcity of CD4^{+}Foxp3^{+} T cells in DIO-associated VAT implicated these cells in metabolic controls, the adoptive transfer model did not. To gain more insight into this issue, we used immunotherapy to possibly reset the diet-induced shifts in VAT T cell constituents, as *in vivo* CD3-specific antibody function depends on the CD4^{+}Foxp3^{+} T cell compartment for its long-term tolerogenic effects[23,33].

We injected mitogenic CD3-specific antibody[34] (10 μg d^{-1} over 5 d) into 14-week-old HFD-fed WT mice. This protocol promotes T cell self-tolerance through global, transient (≤3 weeks) T cell depletion, paralleled by a selective increase of CD4^{+}Foxp3^{+} T cell pools in sites of tissue inflammation[23,33]. Nine weeks after CD3-specific antibody treatment, HFD mice had near lean levels of CD4^{+}Foxp3^{+} T cells in VAT (**Fig. 5a**). Treatment improved fasting glucose and insulin levels and greatly improved glucose tolerance and insulin sensitivity (**Fig. 5b–d**). There was a transient weight loss, lasting 3–4 weeks after CD3-specific antibody injection (**Fig. 5e**). This was probably attributable to the cytokine storm after initial T cell activation, with TNF-α a major mediator[35,36], as the differences in body weight, adipocyte hypertrophy, food intake, CO_2 production and O_2 consumption disappeared over the following weeks on continued HFD (**Fig. 5e** and **Supplementary Fig. 6d**). CD3-specific antibody–mediated normalizing effects on insulin resistance and glucose tolerance emerged 3–4 weeks after injection and lasted the entire observation period (≥4 months, **Supplementary Fig. 7a–d**), despite continued exposure to the hypercaloric diet. We observed a similar but slightly less effective impact on metabolic parameters after treatment of leptin-deficient *ob/ob* mice with CD3-specific antibody (**Supplementary Fig. 7e–i**). Reduced efficiency of CD3-specific antibody in *ob/ob* mice correlated with reduced restoration of T regulatory cell numbers in VAT (**Supplementary Fig. 7e**), probably owing to the multiple immune abnormalities associated with leptin deficiency[37].

Adverse effects of the cytokine storm may limit the utility of intact CD3-specific antibody therapy. We therefore tested the non-mitogenic F(ab′)$_2$ fragment of CD3-specific antibody[34]. Injection of 150 μg of F(ab′)$_2$ per d over 5 d resulted in long-term improvements of glucose tolerance and fasting glucose and insulin concentrations (**Fig. 5f**) without weight loss (**Fig. 5g**) in HFD-fed mice. F(ab′)$_2$ treatment also restored CD4^{+}Foxp3^{+} T cell numbers in VAT (**Fig. 5h**). Notably, the IFN-γ^{+} T$_H$1 bias and the abundance of other VAT cytokines measured remained unchanged by F(ab′)$_2$ therapy (**Fig. 5i,j**), again pointing to, but not proving, that restoration of VAT T regulatory cells improves long-term glucose and insulin homeostasis.

CD4^{+}Foxp3^{+} T cells can induce M2 AAMs[12], which secrete IL-10 and protect against insulin resistance[38]. To determine whether the restoration of VAT regulatory T cells by CD3-specific antibody immunotherapy did, in fact, generate IL-10–secreting M2

macrophages, we established cytokine profiles of M2 macrophages on the basis of surface staining of MMR. We distinguished three F4/80$^+$ macrophage populations in VAT of both HFD- and NCD-fed mice: MMR$^-$, MMR^{lo} and MMR^{hi} macrophages (**Fig. 6a**). Only MMR^{hi} macrophages expressed IL-10; MMR^{lo} macrophages were the largest source of MCP-1, and MMR$^-$ macrophages expressed MCP-1 and TNF-α, likely representing classical M1 macrophages (**Fig. 6b**).

Notably, diet had little effect on these cytokine patterns (**Fig. 6b**). However, HFD-fed mice generated more MMR$^-$ macrophages and less IL-10–secreting MMR^{hi} macrophages compared to NCD-fed mice (**Fig. 6a**). F(ab′)$_2$ therapy increased the MMR^{hi} pool and reduced the MMR$^-$ pool by 6 weeks after treatment (**Fig. 6c**). This macrophage shift generated an ~300% increase in IL-10 production, as measured in purified VAT macrophages from F(ab′)$_2$–treated DIO mice (**Fig. 6d**). F(ab′)$_2$ therapy seems to have dual functions, increasing both anti-inflammatory T cell and macrophage compartments in VAT.

DISCUSSION

We identified a fundamental role for CD4$^+$ T lymphocytes in the regulation of body weight, adipocyte hypertrophy, insulin resistance and glucose tolerance, implicating these cells in the control of disease progression in DIO and the *ob/ob* form of type 2 diabetes. We revealed the lymphocyte impact with independent models and experiments, including Rag1-null mice, which develop an overtly diabetic phenotype on a HFD.

Our evidence maps T cell–mediated metabolic rescue to both, CD4$^+$Foxp3$^+$ and CD4$^+$Foxp3$^-$ (for example, T$_H$2) T cell compartments. Whereas CD4$^+$Foxp3$^-$ cells affected obesity and insulin resistance, CD4$^+$Foxp3$^+$ cells primarily regulated insulin resistance, although this was not as apparent in our adoptive transfer models, where T$_H$2 cells emerged as regulators of obesity and insulin resistance. Overall, our experiments do not rule out effects of B lymphocytes or VAT-associated innate lymphocyte subsets (for example, NK, NKT, TCRγ/δ or CD4$^-$CD8$^-$TCRα/β$^+$ subsets)[24]. In fact, our preliminary data suggest that B cell deficiency in DIO mice is associated with improved metabolic control (S.W., Y.C., G.P. and H.-M.D. unpublished data).

We primarily focused on mouse models, but our limited human studies support the conclusions we drew from the mouse experiments. VAT of DIO mice and obese humans is characterized by an abnormally high T$_H$1 to Foxp3$^+$ cell ratio; high expression of IFN-γ in human VAT was previously associated with increased waist circumference[17]. IFN-γ is a proinflammatory cytokine, and increased numbers of T$_H$1 cells in VAT may contribute to insulin resistance, an observation supported by improved glucose tolerance in T$_H$1 cell–deficient, IL-12p35–null mice (S.W., Y.C., H.T. and H.-M.D., unpublished data) and in IFN-γ–null mice[39]. We favor a model where a relatively constant pool of CD4$^+$Foxp3$^+$ and T$_H$2 fat-associated T cells gradually fails to limit expanding pools of T$_H$1 cells, leading to a progressively proinflammatory environment that promotes insulin resistance. It is also possible that T regulatory cell function may be suboptimal in the inflammatory VAT environment, as suggested in autoimmune disease models[40]. Factors that drive T$_H$1 cell influx, expansion or both in VAT are unknown but now appear to include antigen-driven expansion, with a role for classical immune elements such as the T$_H$1 chemokine RANTES[18].

The precise mechanisms by which CD4$^+$ T cells affect insulin sensitivity require further study. The induction of IL-10–secreting M2 macrophages represents one potential mechanism, although we ruled out such a role for T cell-derived IL-10. CD4$^+$Foxp3$^+$ T cells induce M2c-type AAMs through production of IL-10 and TGF-β, whereas T$_H$2 T cells can induce M2a-type AMMs[13]. AAMs can regulate insulin resistance through IL-10–mediated reversal of TNF-α–induced insulin resistance[15]. AAMs are present in adipose tissue of lean mice, but, as obesity ensues, there is a shift to proinflammatory M1 macrophages[15]. This shift to M1 macrophages is probably a result of steadily increasing T$_H$1 to Foxp3$^+$ and T$_H$1 to T$_H$2 cell ratios. In fact, we observed increases in VAT M2 macrophages and decreases in M1 macrophages after restoration of CD4$^+$Foxp3$^+$ T cell pools after F(ab′)$_2$ immunotherapy.

CD3-specific antibody is a potent, clinically used immunosuppressant, and a possible therapeutic in type 1 diabetes[34,41]. Its immune effects are reversible, well understood and easily monitored. The data presented here suggest that it may be of use in the treatment of insulin resistance. In such individuals, use of CD3-specific antibody may have multiple benefits, as it is effective in reducing atherosclerotic plaques, common in obesity and insulin resistance syndromes[42]. We observed a similar but slightly less effective course of CD3-specific antibody immunotherapy in diabetic, leptin-deficient *ob/ob* mice. However, leptin affects multiple pathways in the immune response, including TGF-β signaling, T cell homeostasis and macrophage and dendritic cell maturation[43,44]. CD3-specific antibody immunotherapy requires TGF-β secretion by phagocytes, and deficiencies in this pathway may account for somewhat reduced efficiency in leptin-deficient mice[45].

Although we focused on the metabolic roles of lymphocytes in VAT, we cannot rule out lymphocyte impact on insulin resistance in other organs such as the liver. We also cannot rule out a role for CD8$^+$ T cells in disease development. Although transfer studies show that CD8$^+$ T cells in isolation have little impact on obesity and associated insulin resistance, it is possible that, with CD4$^+$ T cell help, CD8$^+$ T cells and possibly the regulatory CD8$^+$ subsets[33] become more active participants.

Our perhaps most unexpected discovery was the TCR V$_\alpha$ bias in DIO OT2 and B6 mice. Antigen-driven T cell selection and expansion in VAT would be the most likely explanation, substantially supported by the failure of exclusively OVA-specific T cells to transfer the protective functions of T$_H$2 and Foxp3$^+$ T cell compartments. Further validation, through identification of candidate adipose tissue epitopes, would imply autoimmunity in obesity, where VAT selective adipocyte death has, in fact, already been described[46].

Collectively, we have shown a previously unknown role for the adaptive immune system in the regulation of obesity, fat distribution and insulin resistance. Our observations identify several T cell populations as physiological regulators in these processes, and they identify VAT-selective, TCR-dependent, cognate immunity as one element driving T cell expansion in VAT. This observation strongly implies that VAT incites active T cell immunity. Work is underway to identify the inciting antigenic epitopes to open a door to globally affordable tolerogenic vaccination strategies against DIO and, possibly, its associated metabolic syndromes, including type 2 diabetes.

METHODS

Methods and any associated references are available in the online version of the paper at http://www.nature.com/naturemedicine/.

Note: Supplementary information is available on the Nature Medicine website.

ACKNOWLEDGMENTS

These studies were supported by the Canadian Institutes of Health Research. Y.C. and G.P. were recipients of scholarships from the Canadian Institutes of Health Research and the Banting & Best Foundation. Antibodies to OT2 TCR heavy and light chain were a gift from D. Philpott (University of Toronto).

AUTHOR CONTRIBUTIONS
S.W. and Y.C. conceived of the study and carried out the bulk of the experiments. G.P., D.T., H.T. and Y.M. performed a number of mouse experiments. R.D., Y.W. and J.Z. provided much of the TCR material, F.M. helped with adipocyte analysis, J.B. and D.D. provided metabolic studies, E.E. and D.W. generated the bulk of human data, S.W. and H.-M.D. wrote the manuscript, and H.-M.D. financed and supervised the project and the peer review process.

COMPETING INTERESTS STATEMENT
The authors declare competing financial interests: details accompany the full-text HTML version of the paper at http://www.nature.com/naturemedicine/.

Published online at http://www.nature.com/naturemedicine/.
Reprints and permissions information is available online at http://npg.nature.com/reprintsandpermissions/.

1. Kahn, S.E., Hull, R.L. & Utzschneider, K.M. Mechanisms linking obesity to insulin resistance and type 2 diabetes. *Nature* **444**, 840–846 (2006).
2. Déspres, J.P. & Lemieux, I. Abdominal obesity and metabolic syndrome. *Nature* **444**, 881–887 (2006).
3. Dahabreh, I.J. Meta-analysis of rare events: an update and sensitivity analysis of cardiovascular events in randomized trials of rosiglitazone. *Clin. Trials* **5**, 116–120 (2008).
4. Hanson, R.L., Imperatore, G., Bennett, P.H. & Knowler, W.C. Components of the 'metabolic syndrome' and incidence of type 2 diabetes. *Diabetes* **51**, 3120–3127 (2002).
5. Hotamisligil, G.S. Inflammation and metabolic disorders. *Nature* **444**, 860–867 (2006).
6. Kim, J.Y. *et al.* Obesity-associated improvements in metabolic profile through expansion of adipose tissue. *J. Clin. Invest.* **117**, 2621–2637 (2007).
7. Furuhashi, M. *et al.* Adipocyte/macrophage fatty acid-binding proteins contribute to metabolic deterioration through actions in both macrophages and adipocytes in mice. *J. Clin. Invest.* **118**, 2640–2650 (2008).
8. Kanda, H. *et al.* MCP-1 contributes to macrophage infiltration into adipose tissue, insulin resistance, and hepatic steatosis in obesity. *J. Clin. Invest.* **116**, 1494–1505 (2006).
9. Yuan, M. *et al.* Reversal of obesity- and diet-induced insulin resistance with salicylates or targeted disruption of Ikkβ. *Science* **293**, 1673–1677 (2001).
10. Weisberg, S.P. *et al.* CCR2 modulates inflammatory and metabolic effects of high-fat feeding. *J. Clin. Invest.* **116**, 115–124 (2006).
11. Odegaard, J.I. *et al.* Macrophage-specific PPARγ controls alternative activation and improves insulin resistance. *Nature* **447**, 1116–1120 (2007).
12. Tiemessen, M.M. *et al.* $CD4^+CD25^+Foxp3^+$ regulatory T cells induce alternative activation of human monocytes/macrophages. *Proc. Natl. Acad. Sci. USA* **104**, 19446–19451 (2007).
13. Martinez, F.O., Sica, A., Mantovani, A. & Locati, M. Macrophage activation and polarization. *Front. Biosci.* **13**, 453–461 (2008).
14. Cintra, D.E. *et al.* Interleukin-10 is a protective factor against diet-induced insulin resistance in liver. *J. Hepatol.* **48**, 628–637 (2008).
15. Lumeng, C.N., Bodzin, J.L. & Saltiel, A.R. Obesity induces a phenotypic switch in adipose tissue macrophage polarization. *J. Clin. Invest.* **117**, 175–184 (2007).
16. Rausch, M.E., Weisberg, S., Vardhana, P. & Tortoriello, D.V. Obesity in C57BL/6J mice is characterized by adipose tissue hypoxia and cytotoxic T-cell infiltration. *Int. J. Obes. (Lond.)* **32**, 451–463 (2008).
17. Kintscher, U. *et al.* T-lymphocyte infiltration in visceral adipose tissue. a primary event in adipose tissue inflammation and the development of obesity-mediated insulin resistance. *Arterioscler. Thromb. Vasc. Biol.* **28**, 1304–1310 (2008).
18. Wu, H. *et al.* T-cell accumulation and regulated on activation, normal T cell expressed and secreted upregulation in adipose tissue in obesity. *Circulation* **115**, 1029–1038 (2007).
19. Baker, F.J., Lee, M., Chien, Y.H. & Davis, M.M. Restricted islet-cell reactive T cell repertoire of early pancreatic islet infiltrates in NOD mice. *Proc. Natl. Acad. Sci. USA* **99**, 9374–9379 (2002).
20. Turner, S.J., Doherty, P.C., McCluskey, J. & Rossjohn, J. Structural determinants of T-cell receptor bias in immunity. *Nat. Rev. Immunol.* **6**, 883–894 (2006).
21. Oksenberg, J.R. *et al.* Limited heterogeneity of rearranged T-cell receptor V α transcripts in brains of multiple sclerosis patients. *Nature* **345**, 344–346 (1990).
22. Jenkins, R.N., Nikaein, A., Zimmermann, A., Meek, K. & Lipsky, P.E. T cell receptor V β gene bias in rheumatoid arthritis. *J. Clin. Invest.* **92**, 2688–2701 (1993).
23. Belghith, M. *et al.* TGF-β–dependent mechanisms mediate restoration of self-tolerance induced by antibodies to CD3 in overt autoimmune diabetes. *Nat. Med.* **9**, 1202–1208 (2003).
24. Caspar-Bauguil, S. *et al.* Adipose tissues as an ancestral immune organ: site-specific change in obesity. *FEBS Lett.* **579**, 3487–3492 (2005).
25. Szabo, S.J. *et al.* A novel transcription factor, T-bet, directs T_H1 lineage commitment. *Cell* **100**, 655–669 (2000).
26. Barnden, M.J., Allison, J., Heath, W.R. & Carbone, F.R. Defective TCR expression in transgenic mice constructed using cDNA-based α- and β-chain genes under the control of heterologous regulatory elements. *Immunol. Cell Biol.* **76**, 34–40 (1998).
27. Padovan, E. *et al.* Expression of two T cell receptor α chains: dual receptor T cells. *Science* **262**, 422–424 (1993).
28. Fontenot, J.D., Rasmussen, J.P., Gavin, M.A. & Rudensky, A.Y. A function for interleukin 2 in Foxp3-expressing regulatory T cells. *Nat. Immunol.* **6**, 1142–1151 (2005).
29. Awasthi, A. *et al.* A dominant function for interleukin 27 in generating interleukin 10–producing anti-inflammatory T cells. *Nat. Immunol.* **8**, 1380–1389 (2007).
30. Jankovic, D. *et al.* Single cell analysis reveals that IL-4 receptor/Stat6 signaling is not required for the *in vivo* or *in vitro* development of $CD4^+$ lymphocytes with a T_H2 cytokine profile. *J. Immunol.* **164**, 3047–3055 (2000).
31. Shimoda, K. *et al.* Lack of IL-4-induced T_H2 response and IgE class switching in mice with disrupted *Stat6* gene. *Nature* **380**, 630–633 (1996).
32. Kaplan, M.H., Schindler, U., Smiley, S.T. & Grusby, M.J. Stat6 is required for mediating responses to IL-4 and for development of T_H2 cells. *Immunity* **4**, 313–319 (1996).
33. Bisikirska, B., Colgan, J., Luban, J., Bluestone, J.A. & Herold, K.C. TCR stimulation with modified anti-CD3 mAb expands $CD8^+$ T cell population and induces $CD8^+CD25^+$ Tregs. *J. Clin. Invest.* **115**, 2904–2913 (2005).
34. Chatenoud, L. & Bluestone, J.A. CD3-specific antibodies: a portal to the treatment of autoimmunity. *Nat. Rev. Immunol.* **7**, 622–632 (2007).
35. Alegre, M. *et al.* Acute toxicity of anti-CD3 monoclonal antibody in mice: a model for OKT3 first dose reactions. *Transplant. Proc.* **22**, 1920–1921 (1990).
36. Alegre, M. *et al.* Hypothermia and hypoglycemia induced by anti-CD3 monoclonal antibody in mice: role of tumor necrosis factor. *Eur. J. Immunol.* **20**, 707–710 (1990).
37. Claycombe, K., King, L.E. & Fraker, P.J. A role for leptin in sustaining lymphopoiesis and myelopoiesis. *Proc. Natl. Acad. Sci. USA* **105**, 2017–2021 (2008).
38. Zeyda, M. & Stulnig, T.M. Adipose tissue macrophages. *Immunol. Lett.* **112**, 61–67 (2007).
39. Rocha, V.Z. *et al.* Interferon-γ, a T_H1 cytokine, regulates fat inflammation: a role for adaptive immunity in obesity. *Circ. Res.* **103**, 467–476 (2008).
40. Korn, T. *et al.* Myelin-specific regulatory T cells accumulate in the CNS but fail to control autoimmune inflammation. *Nat. Med.* **13**, 423–431 (2007).
41. Herold, K.C. *et al.* Anti-CD3 monoclonal antibody in new-onset type 1 diabetes mellitus. *N. Engl. J. Med.* **346**, 1692–1698 (2002).
42. Steffens, S. & Mach, F. Adiponectin and adaptive immunity: linking the bridge from obesity to atherogenesis. *Circ. Res.* **102**, 140–142 (2008).
43. Macia, L. *et al.* Impairment of dendritic cell functionality and steady-state number in obese mice. *J. Immunol.* **177**, 5997–6006 (2006).
44. Kümpers, P. *et al.* Leptin is a coactivator of TGF-β in unilateral ureteral obstructive kidney disease. *Am. J. Physiol. Renal Physiol.* **293**, F1355–F1362 (2007).
45. Perruche, S. *et al.* CD3-specific antibody–induced immune tolerance involves transforming growth factor-β from phagocytes digesting apoptotic T cells. *Nat. Med.* **14**, 528–535 (2008).
46. Strissel, K.J. *et al.* Adipocyte death, adipose tissue remodeling, and obesity complications. *Diabetes* **56**, 2910–2918 (2007).

ONLINE METHODS

Mice. We purchased WT C57BL/6 mice, *ob/ob*, Rag1-null, IL-10-null, STAT6-null, Foxp3-eGFP and OT2 mice from Jackson Laboratories, and we maintained them in our vivarium in a pathogen-free, temperature controlled, 12-h light and dark cycle environment. The mice received either NCD or HFD (Research Diets, 60 kcal% fat for the HFD), from 6 weeks of age on. All studies used males under approved protocols and in agreement with animal ethics guidelines of the Animal Care Committee at the Hospital for Sick Children, Research Institute.

Cell transfer experiments. We isolated splenocytes from 8-week-old B6 NCD-fed mice as previously described[43], and we purified $CD4^+$ and $CD8^+$ T cells (>95%, Easy Sep, StemCell Technologies). We gave 12-week-old HFD-fed Rag1-null mice 5×10^6 T cells intraperitoneally.

Diet and metabolic studies. We weighed all WT and knockout DIO males regularly. After 8 weeks on HFD, we measured fasting blood glucose and insulin concentrations (Crystal Chem ELISA). For glucose tolerance tests, we gave fasted (16 h) mice 0.75–1 g glucose per kg body weight; for ITT mice, we gave them 0.75 U per kg body weight human regular insulin (Eli Lilly) (2 U per kg in *ob/ob* mice). For VAT to SAT ratios, we pooled and averaged the weights of VAT and SAT fat pads. We measured fat cell diameter with the straight-line tool in Image SXM software and quantified at least 200 fat cells each from two different tissue sections per mouse.

Oxymax and food intake studies. We placed mice in individual metabolic chambers with free access to water and pre-weighed food, measuring O_2 consumption, CO_2 output and heat at 15-min intervals over 22 h by indirect calorimetry (Oxymax System, Columbus Instruments). We normalized all measurements to body weight. Similar studies comparing DIO WT and DIO Rag1-null mice were performed at Jackson Laboratories.

Fat-associated T cell isolation. We systemically perfused isoflurane-anesthetized mice with PBS, dissected epididymal VAT and inguinal SAT pads (carefully avoiding lymph nodes), mashed the tissue and digested with collagenase (Sigma, 0.2 mg ml^{-1} in DMEM for 45 min at 37 °C, with manual shaking every 5 min). We pelleted the digests and filtered them (40-μm filter) to enrich fat-associated T cells.

Flow cytometry and ELISAs. We stained splenocytes or fat-associated T cells for 30 min with commercial (eBiosciences) antibodies to the following proteins (dilutions in parentheses): CD3 (1 in 150), CD4 (1 in 200), IL-17 (1 in 150), IFN-γ (1 in 100), Foxp3 (1 in 100), IL-10 (1 in 100), BD Biosciences provided GATA-3 (prediluted) or CD8 (1 in 300). We labeled macrophages with phycoerythrin-conjugated antibody to F4/80 (1 in 100) (eBioscience) and sorted them. We used allophycocyanin-streptavidin (1 in 100) (eBioscience) to label biotinylated MMR (1 in 50) (R&D Systems). For intracellular staining of T cells, we incubated the cells with phorbol myristate acetate (PMA) (50 ng ml^{-1}) and ionomycin (750 ng ml^{-1}) for 14 h in HL-1 medium at 37 °C, adding Golgistop (BD Bioscience) for the last 11 h before FACS plot analysis with FlowJo software.

We measured serum concentrations of TNF-α, IL-6, adiponectin, leptin and resistin by ELISA in a blinded fashion (AssayGate). We stimulated isolated fat-associated T cells (200×10^3) with plate-bound antibody to CD3 (1 μg ml^{-1}) plus antibody to CD28 (0.25 μg ml^{-1}) for 72 h in HL-1 medium (Lonza). We sorted $F4/80^+$ macrophages (150×10^3) from adipose stromal vascular cells and stimulated them with LPS (100 ng ml^{-1}, 24 h, 10% FBS in HL-1 medium). For macrophage subset studies, we stimulated 1×10^5 cells per macrophage subset *ex vivo*. We followed manufacturer's protocols for all ELISAs: IFN-γ, IL-10, IL-4 (BD Bioscience), IL-17, IL-13 (R&D Systems), MCP-1 and TNF-α (eBioscience).

Antibody to CD3. We injected 10 μg CD3-specific antibody (clone 145-2C11, BD Biosciences) or purified hamster IgG isotype control (eBioscience) in 100 μl PBS intraperitoneally for 5 consecutive d. For $F(ab')_2$ experiments, we injected 150 μg of $F(ab')_2$ (Bio X Cell) or isotype control (Bio X Cell) in 150 μl of PBS intraperitoneally for 5 consecutive d. All mice survived without obvious complications.

Histology and immunohistochemistry. We fixed VAT and SAT fat pads for 24 h in 10% buffered formalin. Two researchers, including one certified pathologist (D.W.), analyzed H&E stained samples in a blinded fashion. We obtained human VAT from mesenteric tissue of surgically removed colons from patients with colon cancer who gave informed consent under an approved protocol set by the Stanford Internal Review Board for Human Subjects. For immunohistochemistry, we used paraffin-embedded sections subjected to antigen retrieval in pH 6 (Diva Decloaker, Biocare Medical) with the following antibody dilutions: 1 in 100 mouse antibody to Foxp3 (Abcam), 1 in 100 rabbit antibody to Tbet (Santa Cruz) and 1 in 100 rabbit antibody to CD14 (Atlas). Color was produced with Ferangi blue (Biocare Medical) and diaminobenzidine (Vector labs). We determined Tbet to Foxp3 ratios by counting at least 200 stained cells from two different levels of tissue. There was no tumor infiltration in the areas examined.

T cell receptor studies. We sorted the following cell subsets by FACS into RNALater stabilization reagent (Qiagen): ~100,000 splenic- and ~10,000 VAT-derived, rearranged OT2 T cells ($CD4^+$ transgenic TCR V_α^{lo}) from pooled DIO OT2 mice ($n = 5$; 16 weeks old), $\sim 5 \times 10^6$ splenic- and ~50,000 VAT-derived WT T cells ($CD4^+$ TCR $V_\beta{}^+$ $NK1.1^{neg}$) from pooled DIO B6 mice ($n = 10$; 16 weeks of age) and WT B6 mice ($n = 18$; 16 weeks of age). We extracted RNA with the RNA Mini kit (Qiagen) and generated complementary DNA by random priming (Qiagen).

We used two sets of nascent degenerate sense variable region primers ($V_{\alpha 1}$–$V_{\alpha 20}$), with antisense primers in the constant region for nested-amplification of TCRα cDNAs by standard procedures. We analyzed PCR products from the second amplification round on precast agarose gels (Invitrogen). For high-resolution analysis, we ran OT2 second-round products, generated with 5′-carboxyfluorescein–labeled constant region primers, on an ABI Prism 3100 Genetic Analyzer and analyzed profiles with GeneScan software v3.7 (ABI).

Statistical analyses. We assessed statistical significance between two means by Mann-Whitney and unpaired t tests, using the Welch correction on sample sizes smaller than six. Curves were analyzed by two-way ANOVA. Statistical significance was two-tailed and set at 5%.

S1

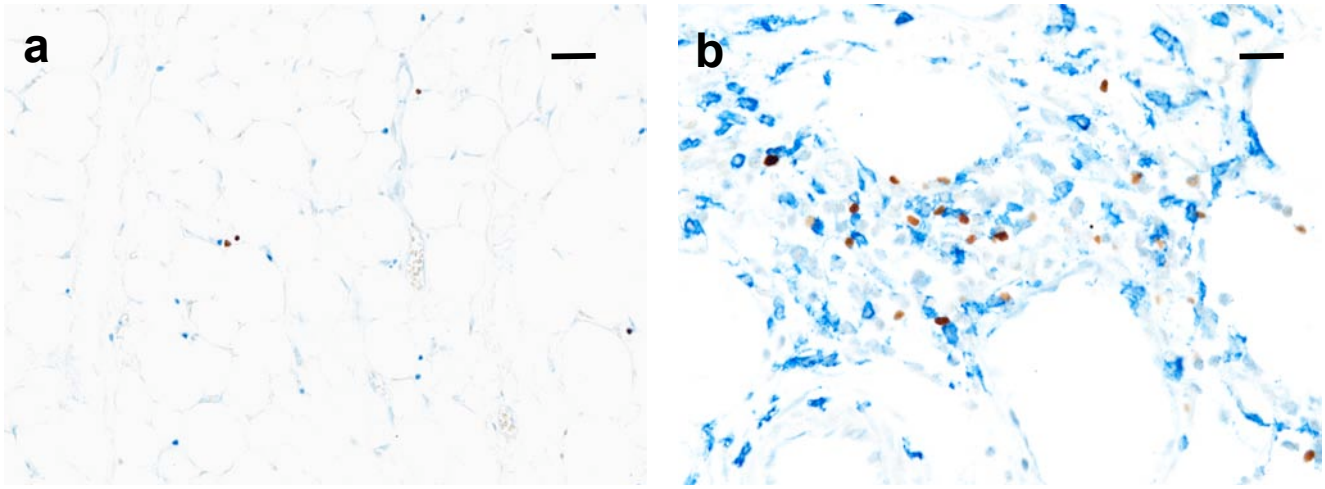

S1a) T-bet (blue) and Foxp3 (brown) cells are scattered throughout adipose tissue (magnification 200X, bar: 50 μm). **b)** Foxp3 (brown) cells are often found in close contact with CD14+ antigen presenting cells (blue, magnification 400X, bar: 25 μm).

S2

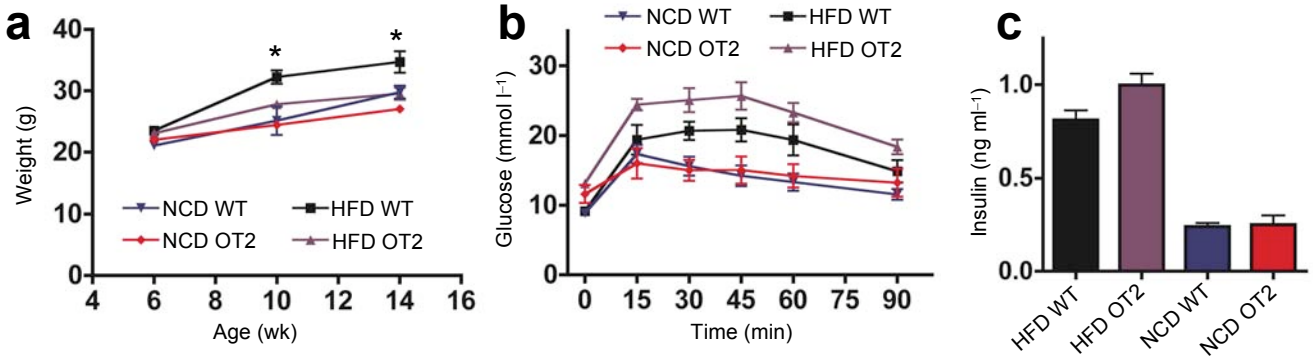

S2a) Body weights of B6 or B6.OT2 mice on NCD or HFD (n=5, *p<0.05, t-test at each time). **b**) Glucose tolerance of NCD WT, NCD B6.OT2 mice and HFD WT, HFD B6.OT2 mice (n=5, p>0.2, 2-way AVONA). **c)** Fasting insulin levels of NCD and HFD WT and B6.OT2 mice (n=5/group).

S3

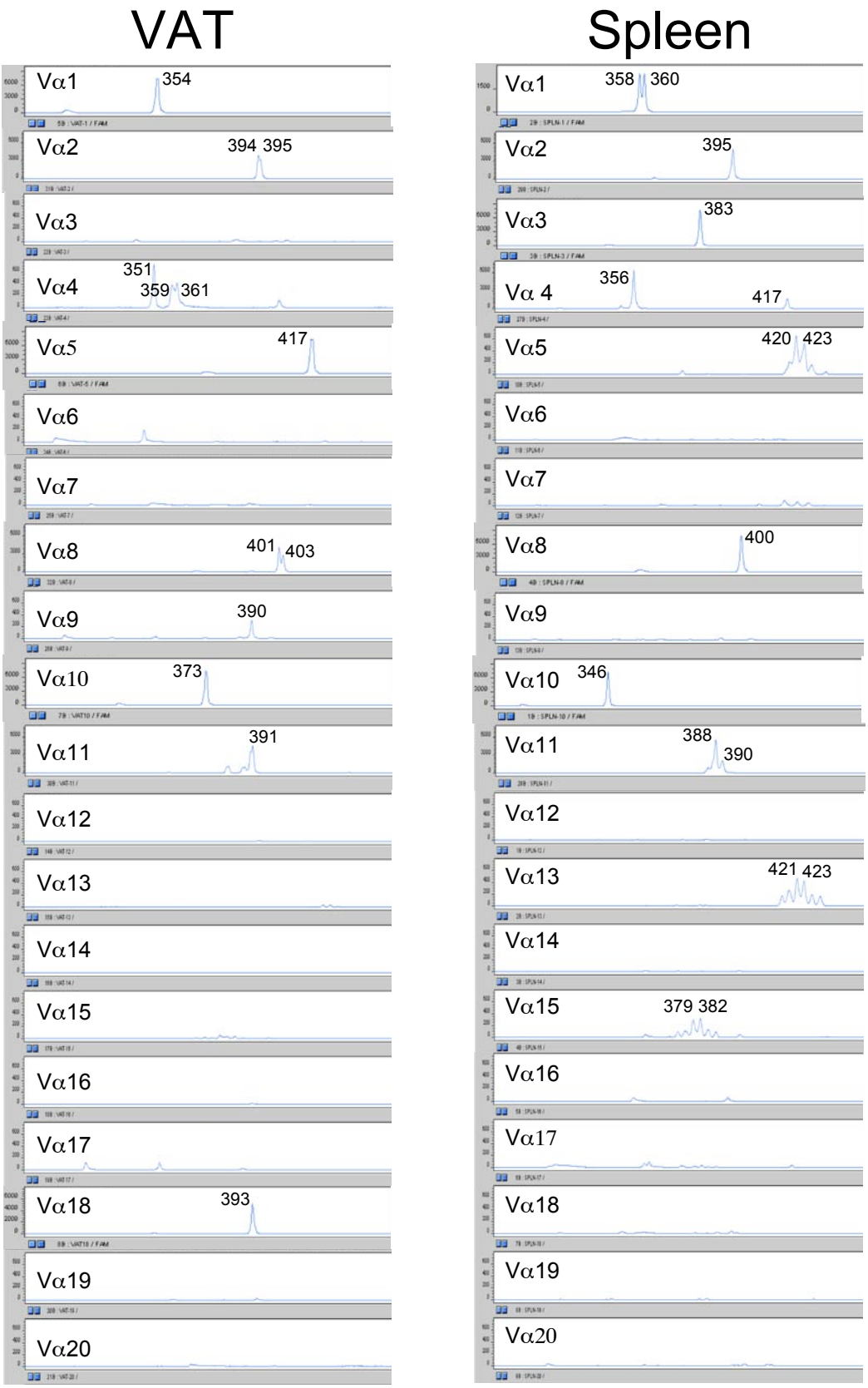

S3) TCR-Vα spectra-typing for Vα1-20 of CD4+ T cells with re-rearranged TCRα sorted from HFD OT2 spleen and VAT (peak numbers = size (bp) of PCR product (x-axis), y-axis: florescence intensity. Area under peak: relative proportion of the clone within the particular Vα family.

S4

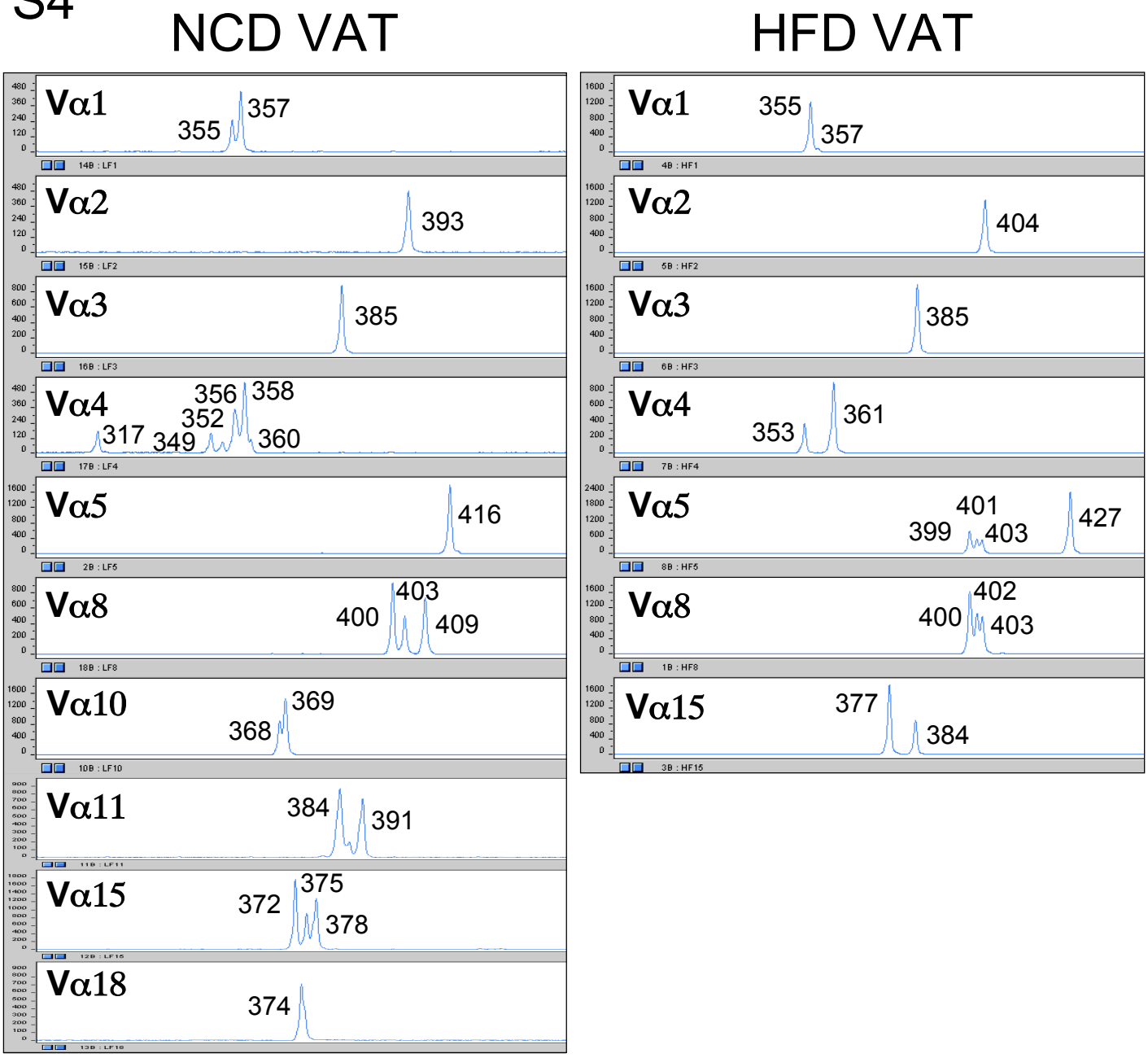

S4) TCR-Vα spectra-typing of WT NCD (Vα1-5, Vα8, Vα10, Vα11, Vα15, Vα18) and HFD B6 mice (Vα1-5, Vα8 and Vα15). See Fig. S3 for labels.

S5

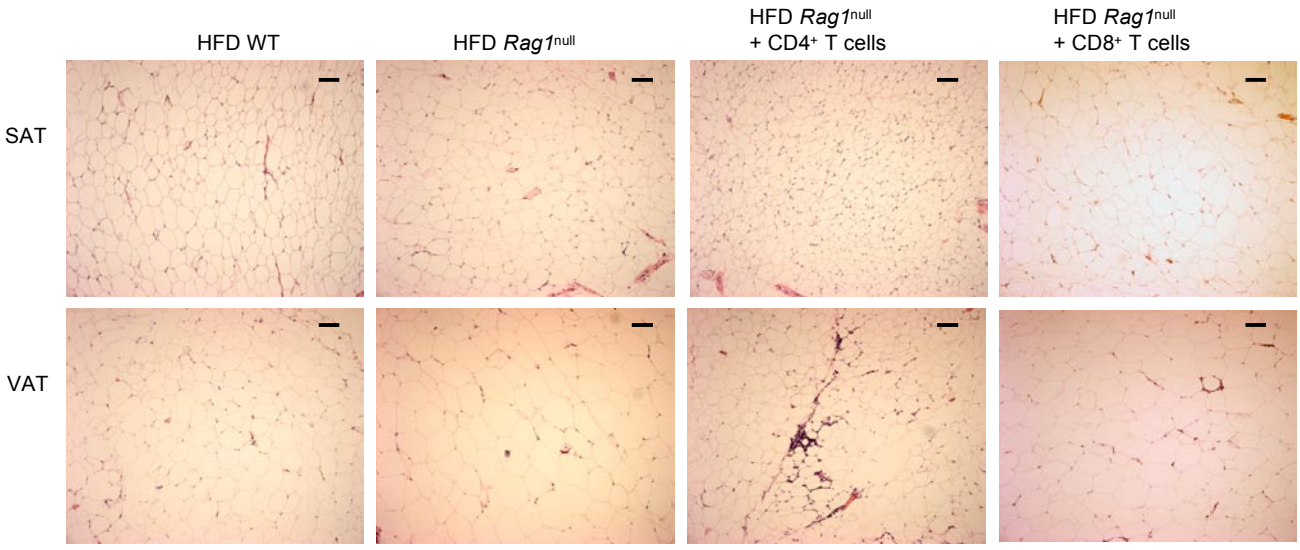

S5) Representative H&E stained tissue from SAT and VAT of 14-16 wk old HFD WT, or HFD RAG^{null} mice that had received 5x10^6 CD4+ or CD8+ T cells 4 wk previously (bars: 100 μm).

S6

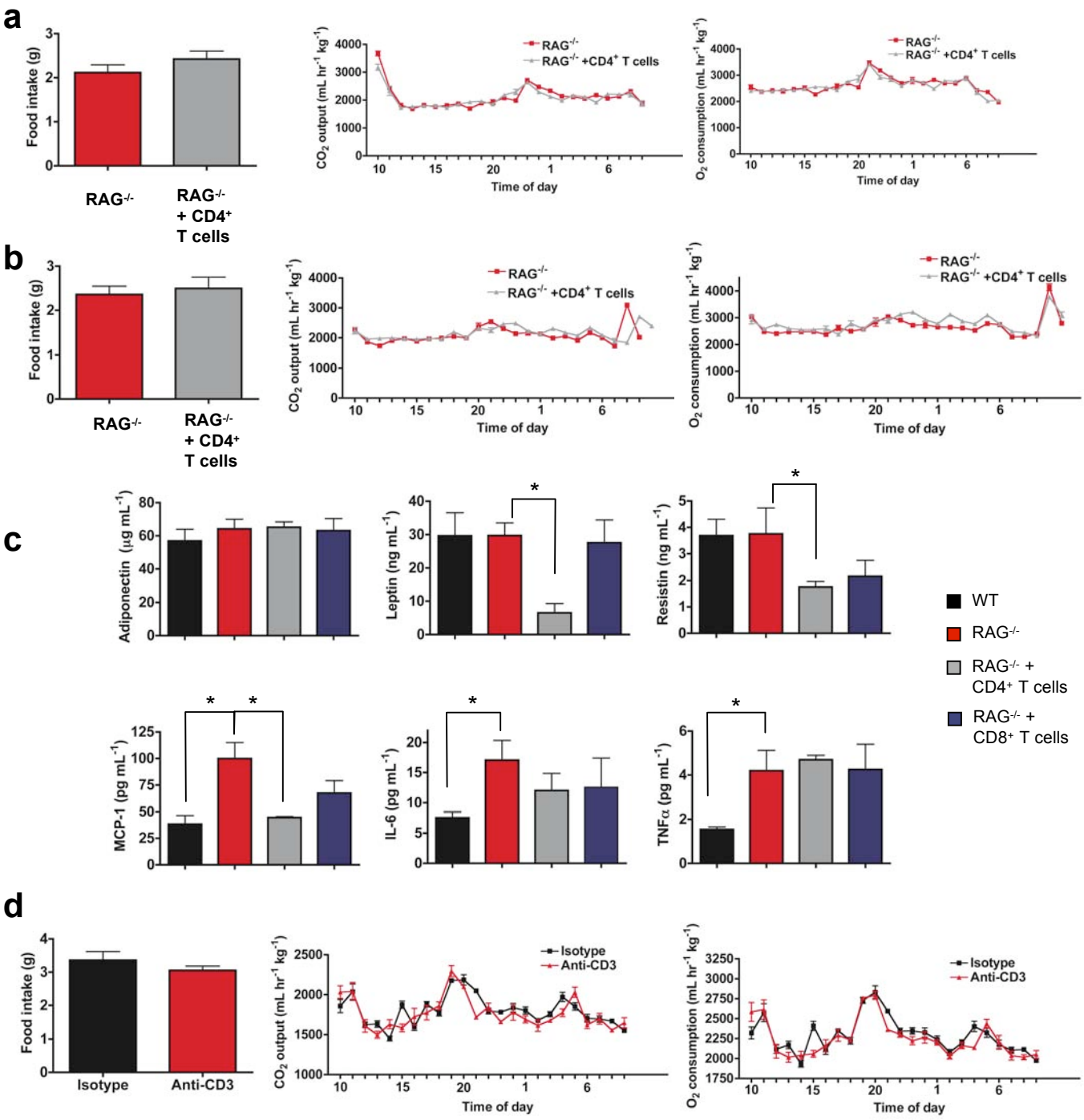

S6a, b) No difference in food intake (left panel), CO_2 output (middle panel) or O_2 consumption over 24 hr, one wk (**a**) or two wk (**b**) following transfer of $5x10^6$ CD4+ T cells into HFD RAG^{null} mice (n=4/group)**. c**) Serum levels of adiponectin, leptin, resistin, MCP-1, IL-6, and TNF-α from 16 wk old HFD WT, HFD RAG^{null}, or age matched HFD RAG^{null} mice, previously transferred with $5x10^6$ CD4+ or CD8+ T cells (n=3-6/bar, *p<0.05, t-test). **d)** 24 hr food intake, CO_2 output and O_2 consumption in 23 wk old HFD B6 mice, 9 wk following αCD3.

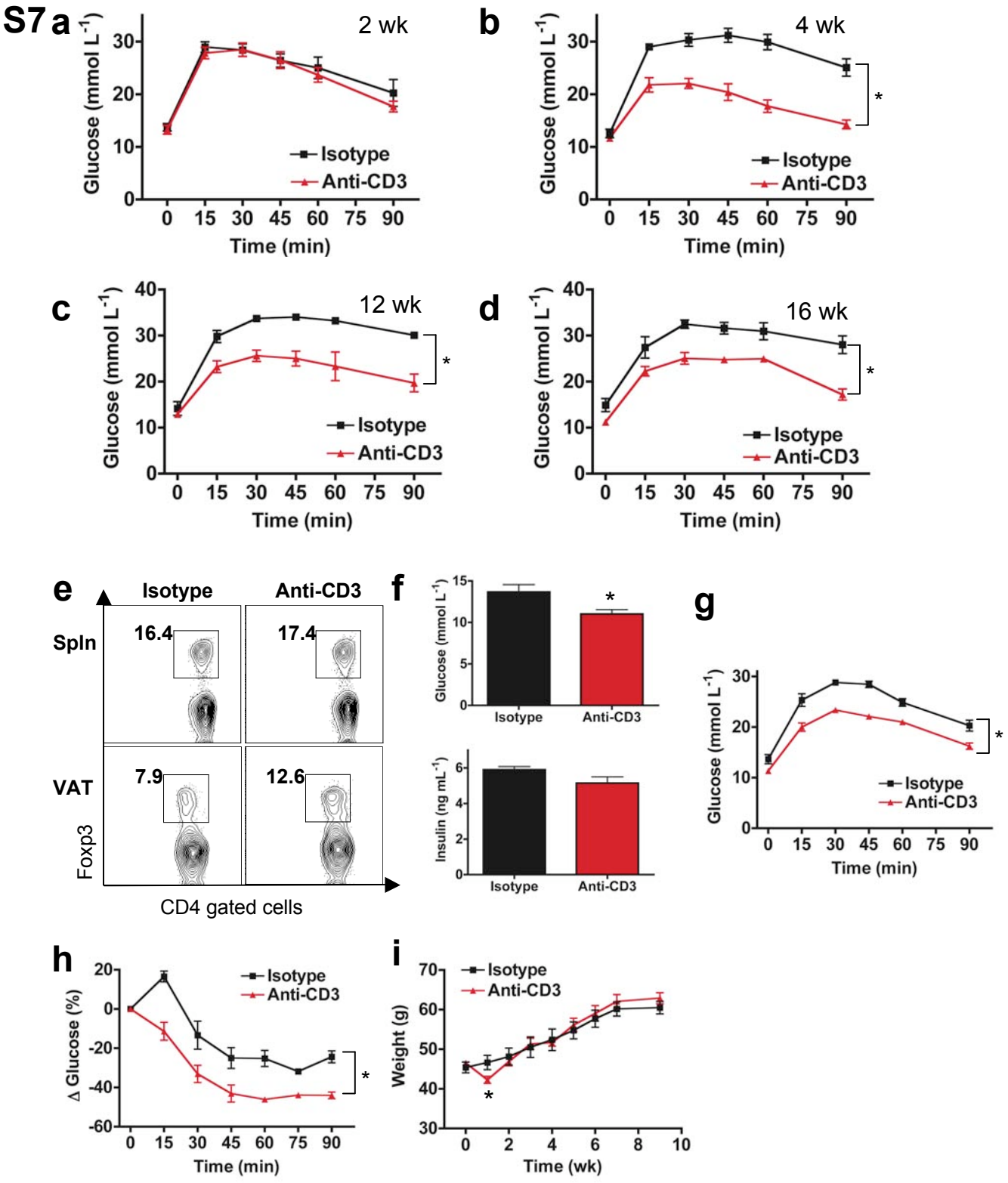

S7a-d) The effects of αCD3 on glucose tolerance in 16 wk old HFD WT B6 mice. (**a**) 2 wk (**b**) 4 wk (**c**) 12 wk and (**d**) 16 wk *post* treatment. Results at 4 wk, 12 wk, and 16 wk are significant (n=5/group, *p<0.03 in all groups, 2-way ANOVA). **S7e-i) αCD3 effects in ob/ob B6 mice. S7e)** Increased CD4+Foxp3+ T cells (%), one of 3 similar experiments. **f**) Fasting glucose (top panel) and insulin (bottom panel) levels in treated or control ob/ob mice (n=8, *p<0.05, t-test). **g**) Improved GTT (n=8, *p<0.03, 2-way ANOVA) and ITT (**h**, n=8, *p<0.05, 2-way ANOVA) in ob/ob mice *post* αCD3. **i**) Weights *post* αCD3 in B6 ob/ob mice.